LANGMUIR

pubs.acs.org/Langmuir Article

Time Evolution and Effect of Dispersant on the Morphology and Viscosity of Water-In-Crude-Oil Emulsions

Diego F. Muriel and Joseph Katz*

Cite This: *Langmuir* 2021, 37, 1725−1742 Read Online

ACCESS | Metrics & More | Article Recommendations | Supporting Information

ABSTRACT: This study examines the time evolution and effects of adding dispersant (Corexit 9500A) at varying concentrations on the microscopic morphology and bulk viscosity of saltwater-in-crude-oil (Louisiana) mechanically mixed emulsions. Rheology is used for measuring the viscoelastic properties and viscosity, the latter at varying shear rates. Microscopy, followed by machine-learning-based analysis, is used for characterizing the size and spatial distribution of the water droplets in the emulsions. Initially, the water droplets appear as a multiscale lattice with a Sauter diameter of 5.3 μm and a polydispersity of 0.43, with small droplets aggregating around large ones. The corresponding bulk viscosity decreases with increasing shear rate from 2 orders of magnitude to 5 times higher than that of the weathered crude oil. After 7 days, the number of submicron droplets increases, the nearest-neighbor distance decreases, indicating preferential aggregation, and the viscosity increases by 56−112% at high shear rates (5−100 s^{-1}). After 14 and 21 days, some droplets coalesce resulting in loss of clusters and a decrease in viscosity. These trends suggest that changes in the aggregation contribute to the variations in viscosity. Subsequent analysis applies previously developed models for the effect of aggregation on the properties of the emulsion. While the reduction in viscosity is predicted by this model, matching of rates requires modification to the assumed relationship between yield stress and interdroplet forces. Adding dispersant without mixing generates Marangoni-driven flows as the water droplets coalesce. In time, part of the water separates, a fraction forms clouds of submicron droplets, and the rest remains unchanged. Mixing dispersant at low concentration with the emulsion accelerates the coalescence and phase separation. The removed water fraction increases with dispersant concentration, reaching 99.6% for a dispersant-to-emulsion concentration of 10^{-3}. The remaining emulsion consists of fine droplets with Newtonian viscosity that is still 4 times higher than that of the fresh crude oil but only 14% higher than that of the weathered oil.

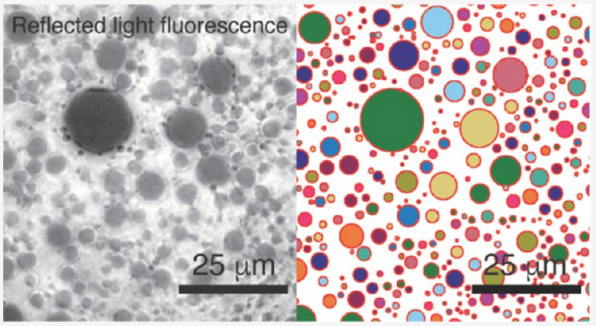

INTRODUCTION

Understanding the physical and chemical processes involved with emulsions is of relevance in multiple fields, from the food industry,[1−3] to pharmaceutical and medical fields.[4] In contrast, environmental studies related to oil spills focus on the formation and fate of oil and water emulsions, especially on how to destabilize them.[5−8] Oil slicks in the open ocean or coastal areas are subjected by breaking waves to shear rates that vary between 5 and 100 1/s.[8,9] The resulting stable water-in-oil (w/o) emulsions contain as high as 60−80% water fractions, which increase the volume of pollutants by 3−5 times and the viscosity by up to 3 orders of magnitude compared to those of the original spilled material.[10−13] These increases are two severe impediments to the environmental remediation of oil spills, resulting in numerous efforts to develop methods for separating the water from the oil by thermal, mechanical, electrical, and chemical techniques.[14,15]

As outlined in detail in the following paragraphs, emulsification of crude oil is facilitated by the formation of interfacial films of naturally present asphaltenes around the water droplets.[16−18] The increase in emulsion viscosity over time has been attributed to changes in the interfacial rigidity.[19−21] In contrast, in laboratory model emulsions, the changes in the macroscopic rheology have been associated with the formation of solid-like networks that aggregate and resist deformation.[22−24] The present study examines the structure of water-in-crude oil emulsions in great detail and correlates them with their macroscopic properties, including shear viscosity, viscoelasticity, and non-Newtonian behavior. The microscopic and macroscopic data are linked through models relating the aggregation to the material behavior. As an environmental remediation method, the application of dispersants after an oil spill is aimed at enhancing the dispersion of the oil by drastically reducing the oil−water interfacial tension.[15] It has

Received: October 13, 2020
Revised: January 11, 2021
Published: January 26, 2021

https://dx.doi.org/10.1021/acs.langmuir.0c02986
Langmuir 2021, 37, 1725−1742

also been shown that chemical dispersants modify the rheology of the interfacial films in emulsions. Hence, the second part of this study examines the effect of mixing the crude oil emulsion with dispersant on the structure and rheology of this emulsion.

This study uses rheometry to measure the viscosity and fluorescence microscopy to examine the size, spatial distribution, and time evolution of the water droplets in water-in-crude oil (Louisiana sweet) metastable emulsions. The results demonstrate that aggregation during the early stages after emulsification increases the viscosity at high shear rates, even if coalescence has not stopped. As coalescence continues and clusters are lost, the viscosity decreases. The Results and Discussion section uses previously developed emulsion models to demonstrate the impact of aggregation on the rheometric properties of the oil. Shortly after adding dispersant to the emulsion without external mixing generates secondary Marangoni-driven flows and droplet coalescence in the parts exposed to the dispersant. Mechanical mixing of the dispersant with the emulsion enhances the phase separation, removing 99.6% of the water for a dispersant-to-emulsion ratio of 1/1000. The remaining emulsion consists mostly of droplets smaller than 1.5 μm at low concentrations. While the resulting Newtonian viscosity is much lower than that of the initial emulsion, it is still 4 times higher than that of fresh crude oil and only 14% higher than that of the weathered oil. Hence, dispersant could be used for decanting of oil. A referenced background about crude oil emulsions, which motivates the present study, is provided next. It is followed by sections describing the methods and experimental procedures, results, discussion, and modeling, as well as conclusions.

BACKGROUND: EMULSIFICATION OF CRUDE OIL

Physically, emulsification involves coalescence and breakup of droplets to create multiple deforming interfaces.[25] Chemically, emulsification involves the migration of surfactants, amphiphilic polymers, or solid particles to the oil−water interface, creating a protective layer.[26] The ability of crude oils to readily emulsify is attributed mainly to the naturally present asphaltenes and resins,[27] where the resins are needed for solvating the asphaltenes[11,28−30] to create a protective viscoelastic interfacial film.[16−18] However, the presence of other solids like crystalline waxes, clays, oceanic particles, corrosion products, and mineral scales may as well lead to the formation of stable water-in-oil (w/o) emulsions.[14,31,32] Regardless of the origin, the interfacial properties dictate in large part the macroscopic properties and the stability of the emulsion.[33−35] Specifically, by irreversibly adsorbing into the oil−water interface,[36−38] asphaltenes impede coalescence either by providing mechanical strength[19,39,40] or sterically by increasing the interfacial adhesion of the droplets when in contact.[41]

As the stable crude oil emulsion ages, its viscosity increases, further complicating the breakup processes.[11] Since interfacial rheology has shown that the elastic modulus of the water−oil interface with asphaltene gradually increases with time, this increase has been attributed mainly to an increase in interfacial rigidity.[17,19−21,39,42] Additionally, thin film drainage experiments have shown that an oil film with asphaltene confined between the water−oil interfaces becomes thicker and more rigid with increasing time.[43−45] Another study[46] has concluded that the asphaltene microstructure is correlated to the rheological response of the film (shear thinning, fracture, and yielding). This trend suggests that morphological heterogeneity affects the film's rheology, which evolves from viscous-dominated to elastic-dominated as it ages.[47]

For model emulsions, e.g., dodecane, silicon oils, glycerol, it has been shown that droplets form solid-like networks that can resist deformation.[22−24,48−51] Consequently, macroscopic rheology is not only modified by the interfacial film properties but by the droplet network structure as well. Even for emulsions having low volume fractions and weakly attractive interactions, the dispersed phase may form aggregates or gels of droplets.[52,53] In these cases, the elasticity of the system could be controlled by the structural features rather than the osmotic pressure, which causes attraction between droplets when the surfactant layer between them is depleted.[54] Such aggregation and its influence on the macroscopic rheology are yet to be shown for crude oil emulsions. While understanding of the microscopic morphology would be fundamental to this study, the available information is quite limited due to difficulties in imaging them in the field and the opacity of crude oil.

Furthermore, considerable attention has been paid to understanding the interfacial rheology for crude oil emulsions upon introduction of dispersant.[5,34,55−63] Several studies have investigated the capacity of dispersants at varying dosages to break the emulsion by spraying it in small containers or based on field experiences.[15,34,64−67] Mixing of fresh crude oil with dispersant drastically reduces the oil−water interfacial tension. At a concentration of about 4%, the reduction is as high as 2 orders of magnitude.[8] Prior studies have shown that once dispersant is added to an emulsion, it displaces the indigenous layers that stabilize the water droplets.[68] Once this elastic layer is compromised, the film drainage and breakup are enhanced,[69] and the water droplets become prone to coalescence. Finally, it is commonly believed that dispersant is ineffective in breaking up aged emulsions, a trait attributed to its inability to modify the interfacial rheology of the associated films.[58] The structural changes to the crude oil emulsion once dispersant is added are unknown.

METHODS

The water-in-crude-oil emulsions are created by mechanically mixing 250 mL of Louisiana sweet crude oil whose properties are listed in Table 1 with 1000 mL of 33 ppt saltwater. The fresh crude oil provided by British Petroleum is a surrogate that has similar properties to that of the MCR252 oil associated with the Deepwater Horizon spill.[70] The properties of this oil have been studied

Table 1. Crude Oil Properties

crude oil	Louisiana, MCR252 surrogate	
	viscosity (mPa·s)	density (kg/m^3)
fresh, μ_{c_f} and ρ_{c_f}	8.24 ± 0.54	875.8 ± 5.8
weathered by dissolution, μ_{c_d} and ρ_{c_d}	10.12 ± 0.50	894.1 ± 6.5
weathered by mixing and dissolution, μ_{c_w} and ρ_{c_w}	29.52 ± 0.36	904.3 ± 3.3
water volume fraction 21 days after mixing with dispersant		
dispersant to emulsion vol. ratio	extracted	remaining (ϕ)
0	0	80.7%
1/4000	93.3%	21.9%
1/2000	98.1%	7.7%
1/1000	99.6%	1.7%

https://dx.doi.org/10.1021/acs.langmuir.0c02986
Langmuir 2021, 37, 1725−1742

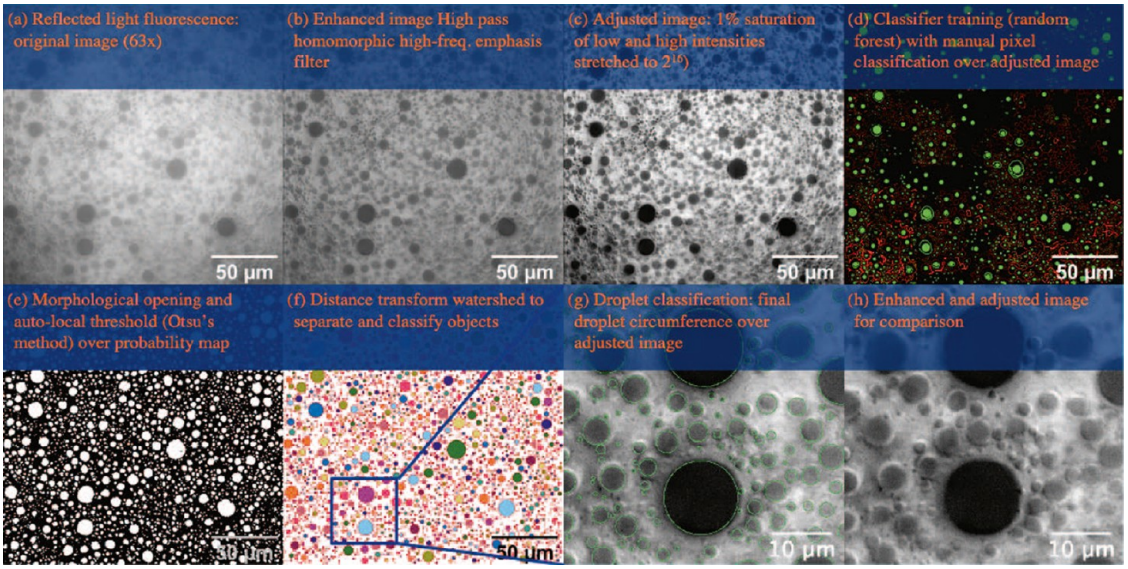

Figure 1. Summary of the application of machine learning to characterize the droplets: (a) original image; (b) enhanced image with background removed; (c) stretched image to 1% of the saturation level; (d) semantic segmentation—manually classified water droplets (green) and oil (red) (e) thresholded image; (f) results of instance segmentation involving distance transform watershed; (g) green lines showing the detected droplets overlaid on a section of the enhanced image; and (h) the enhanced image without the detection lines.

extensively.[71,72] The saturated, aromatic, resins, and asphaltene fractions for fresh MC252 oil are 50.7, 38.9, 10.2, and 0.26, respectively. Since in some of the experiments discussed in this paper the oil undergoes a weathering process, namely, its most volatile components either evaporate or dissolve, published data on the corresponding fractions of weathered oil are 44.2−46.1, 18.4−25.3, 22.6−28.6, and 6.02−8.86.[73] The mixing is performed by an overhead laboratory mixer (XZB Elec Model: DX-120D with a four-blade propeller stirrer) operating at 660 rpm for 22 h in an open 4000 mL glass beaker located inside a fume hood and kept at 20 °C. This procedure allows for evaporation of volatile compounds. Once the mixing is stopped, the emulsion is kept at rest for 1 h before measuring the volume losses. They are as follows: 11.1% of the water does not emulsify (i.e., 889 mL is emulsified), and 14.8% of the oil evaporates (or dissolves) during the mixing process, resulting in an entrained water volume fraction of $\phi = 0.807 \pm 0.033$. The emulsion is then separated into 50 mL samples, which are placed in a series of polypropylene centrifuge tubes. A parallel test verifies that the fraction of water that evaporates during the mixing process is negligible by repeating the procedures using the same saltwater and silicone oil, which does not evaporate.

Four samples have been used for tests performed after 2 h, as well as 7, 14, and 21 days after the mixing. In addition, undisturbed samples have been kept for monitoring the phase separation up to 9 months. Four additional samples are used for studying the effects of mixing the emulsion with Corexit 9500A (Nalco) dispersant at volume fractions of 0, 1/4000, 1/2000, and 1/1000. This mixing is performed for 99 s on day 0 using a vortex mixer (digital VortexGinie2 by Scientific Industries) operating 1500 rpm. The zero fraction emulsion is also "mixed" following the same procedure to use it as control. The dispersant-related mixtures are subsequently kept at rest in polypropylene tubes for tests that begin on day 21. The fraction of water removed from the emulsion is monitored. An additional emulsion sample is placed in a microscope dish, and the dispersant is carefully pipetted on top of it without mixing.

Corexit 9500A, a water-and-oil-soluble dispersant, has been chosen for this study due to its extensive use during the Deepwater Horizon oil spill. Overall, 7×10^6 L of chemical dispersants, including Corexit 9500A and 9527A, were sprayed and injected.[71] The primary components of Corexit 9500A are 18% by weight ionic surfactant dioctyl sodium sulfosuccinate (DOSS), 27% nonionic surfactants, including Span 80, Tween 80, and Tween 85, and 55% carrier solvents, including dipropylene glycol butyl ether and petroleum distillates.[74]

Several methods have been used for examining the morphology of emulsions. Bright-field or differential interference contrast imaging is not suitable for opaque samples. Nuclear magnetic resonance spectroscopy provides the DSD[75−78] but does not resolve the spatial structure of the emulsions. However, owing to the broad-band fluorescence from crude oil, entrained water droplets can be readily detected as black spots in the reflected light fluorescent imaging, enabling measurements of the morphology of emulsions (Figure 1).

For reflected light fluorescence microscopy (Zeiss AxioObserver SIM with Apotome 2), a sample of the top layer of the emulsion is placed in a 9 mm deep and 35 mm diameter FluoroDish Cell Culture Dish (World Precision instruments). The sample is kept small enough such that the cover of the dish does not touch the emulsion. The images are captured using a 16 bit Hamamatsu Orca Flash 4.0 CMOS camera. With a 63× oil immersion objective, the image resolution is 0.10 μm/pixel. Each sample is examined in three different areas, and the results are averaged. A single emulsion sample is examined at high resolutions (maximum of 0.012 μm/pixel) using cryo-scanning electron microscopy (cryo-SEM). The emulsion sample is rapidly frozen in a slush of liquid nitrogen under vacuum and then transferred into a Gatan Alto 2100 Cryo Systems. A series of images of different areas are subsequently captured with no etching or sputter coating.

The viscosity of the emulsions is measured by taking samples from the tubes and placing them in an MCR302 Anton Paar rheometer equipped with a 25 mm diameter parallel plate and a 1.0 mm gap. Each test is performed while increasing the shear rate from 0.01 to 1000 1/s and decreasing the duration from 100 to 1 s, both logarithmically. Ten data points are collected per decade, and six independent tests are performed for each emulsion age and dispersant concentration. Prior to the measurements, the rheometer is calibrated using five viscosity standards covering the relevant range. All of the viscosity measurements of the original oil and the emulsions are performed at 25°C. In addition, as a basis for comparison to the properties of the emulsified oil, the fresh crude oil is also "weathered" following similar exposure history as that occurring during emulsification. First, the 1.25 L of fresh oil is mixed at 660 rpm for 22 h in an open 4000 mL beaker inside a fume hood. Then, the water-soluble compounds are allowed to dissolve by placing 5 mL of samples of the mixed oil on top of 20 mL of water for 21 days. Another sample of fresh oil is placed on top of the water layer for 21

https://dx.doi.org/10.1021/acs.langmuir.0c02986
Langmuir 2021, 37, 1725−1742

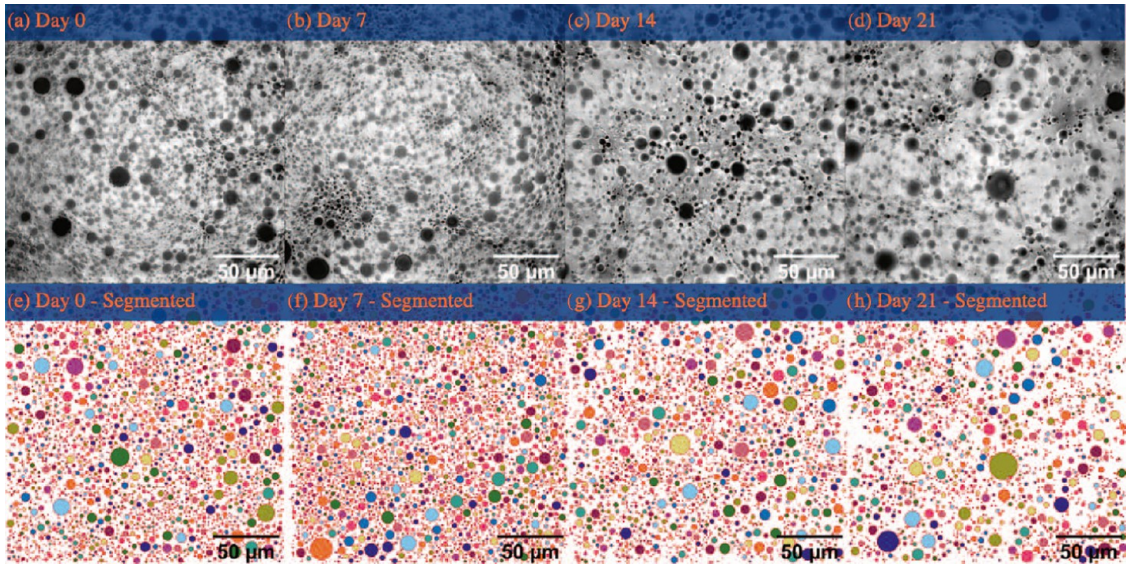

Figure 2. Time evolution of the emulsion, with the top row showing the enhanced fluorescence images and the bottom row showing their corresponding segmented results. Times are as follows: a, e, day 0; b, f, day 7; c, g, day 14; and d, h, day 21.

days without mixing. The viscosity of both oils is subsequently measured.

An additional emulsion created with the same mixing protocol has been tested in the linear viscoelastic region to measure the storage, G', and loss modulus, G'', of the emulsions, shortly after mixing and 8 days later. Since the data indicates that this linear viscoelastic region is satisfied at a shear strain of 5%, it has been chosen for the frequency sweep, ω, ranging from 100 to 0.1 rad/s, decreasing logarithmically. The tests have been performed with the abovementioned rheometer.

Initial attempts to process the images using thresholding-based algorithms have not been successful for the present sections through three-dimensional (3D) samples, which inherently involve nonuniform intensity fields, high water volume fraction, large variations in droplet sizes, and shadows of out-of-plane droplets. Hence, a machine-learning-based pixel-wise classification consisting of the following steps is implemented to determine the droplet diameter and spatial distributions (Figure 1). First, semantic segmentation[79] is used for classifying parts of the images as oil or water droplets. The training features include descriptors of pixel color and intensity, edge sharpness involving a series of filters (Laplacian of Gaussian, Gaussian gradient magnitude, difference of Gaussians), and texture (structure tensor eigenvalues, Hessian of Gaussian eigenvalues). All of the training is performed for 10 different kernel sizes. The random forest, which consists of 100 decision trees and two features per node, is trained for each image based on manually labeled training sets. The training is performed after removing the background illumination using a homomorphic high-frequency emphasis filter (Figure 1a–d). The result of this step is a map of the probability that a certain pixel belongs to water or oil. Second, instance segmentation aimed at defining the droplets starts with morphological opening using a disk element of a 2 pixel radius. Then, autolocal thresholding based on Otsu's method (radius 150[80]) is implemented to obtain a binary mask (Figure 1e). Distance transform watershed is subsequently used to separate overlapping droplets, followed by particle analysis to determine the droplet statistics (Figure 1f–h). Uncertainty estimates based on bootstrapping out-of-bag error[81] show that the maximum misclassification rate varies from 0.09 to 4.57%, corresponding to 1.21 ± 0.01% uncertainty in measuring the droplet diameter. Further details on the uncertainty are provided in Appendix I. The droplet centroids obtained from segmentation are subsequently analyzed to measure the size distributions and nearest-neighbor distance (NND). The latter involves finding five neighboring droplets with the smallest edge-to-edge distances from each droplet. These distances and the corresponding diameters are recorded and used for characterizing the structure of the emulsion. Several definitions are used for describing the characteristic droplet diameter based on the following equation

$$D_{pq} = \left(\frac{\sum_i N_i D_i^p}{\sum_i N_i D_i^q} \right)^{1/(p-q)} \tag{1}$$

where N_i is the total number of droplets with diameters D_i. Hence, D_{10} is the average diameter, D_{30} is the volume mean diameter, and D_{32} is the Sauter diameter. Also, $DV0.5$ is used for the volume median diameter. The polydispersity, P, which quantifies the breadth of the size distribution is defined as

$$P = \frac{1}{DV0.5} \frac{\sum_i^n D_i^3 |DV0.5 - D_i|}{\sum_i^n D_i^3} \tag{2}$$

and the span ratio, R, which also characterizes the size range is defined as

$$R = \frac{DV0.9 - DV0.1}{DV0.5} \tag{3}$$

with $DV0.9$ and $DV0.1$ referring to 90 and 10% of the water volume, respectively, contained in droplets smaller than this value.

RESULTS AND DISCUSSION

Relationship between Aggregation and Viscosity. Figure 2 demonstrates the evolution of the microscopic structure of the water-in-oil (w/o) emulsions without

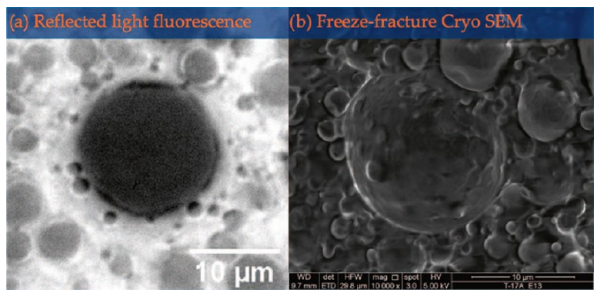

Figure 3. Evidence of small (~1 μm) droplets aggregating around larger ones: (a) fluorescence microscopy and (b) freeze-fracture cryo-scanning electron microscopy.

https://dx.doi.org/10.1021/acs.langmuir.0c02986
Langmuir 2021, 37, 1725−1742

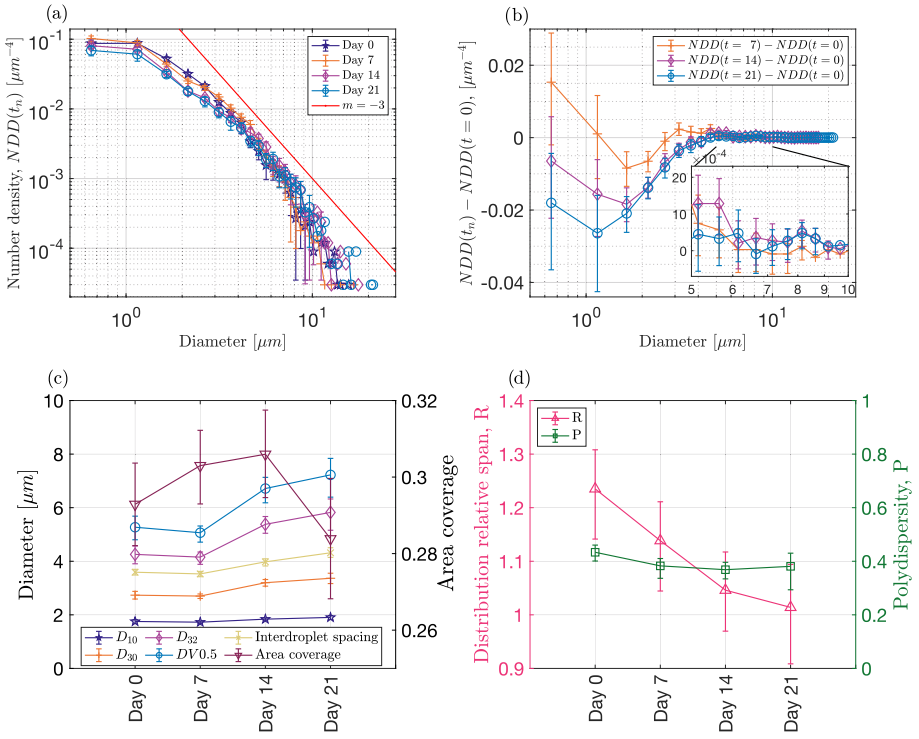

Figure 4. Time evolution of droplet size distributions: (a) number density distributions (NDDs); (b) changes in the NDD between the indicated days and day 0, with the inset highlighting the large droplet data; (c) average droplet statistics, including D_{10}, D_{30}, D_{32}, and $DV0.5$, interdroplet spacing, namely, the square root of the area divided by the number of droplets, and area coverage, i.e., the area fraction occupied by water; and (d) relative span and polydispersity (eqs 2 and 3).

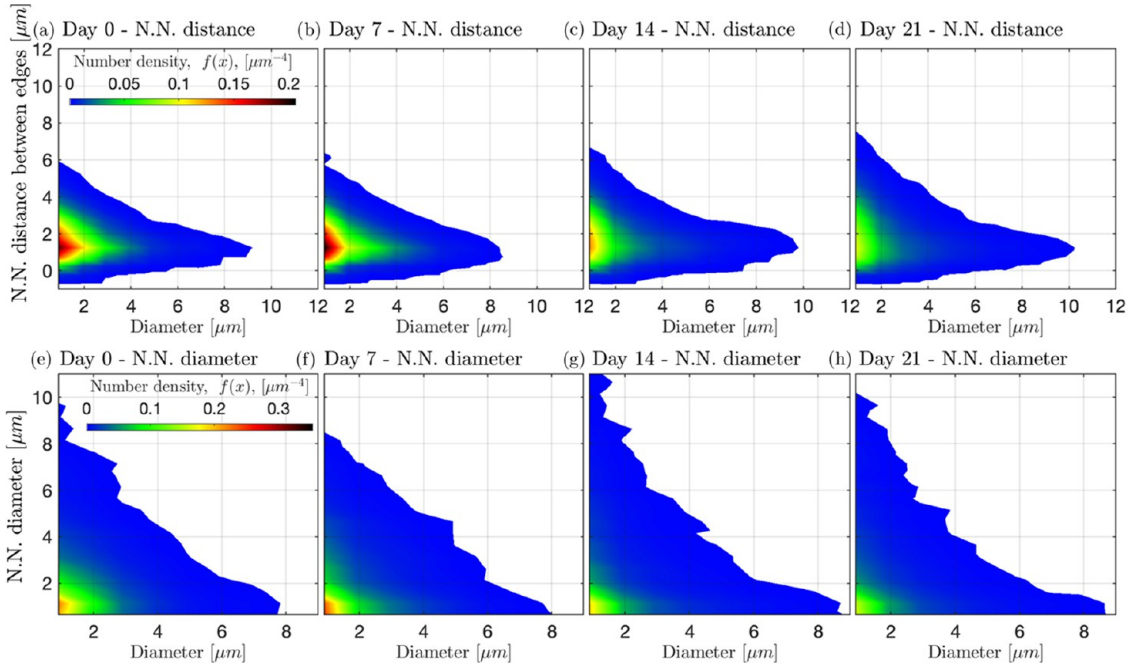

Figure 5. (a–d) Time evolution of the number density of edge-to-edge nearest-neighbor distance between droplets for varying droplet diameters; and (e–h) the corresponding diameters of the nearest neighbors.

dispersant during 21 days. The first row shows the enhanced images, and the second row shows their corresponding segmented graphic depiction. In all cases, the emulsion is polydisperse, with small diameter droplets aggregating around larger ones. While difficult to observe in this figure, this aggregation is evident from the images presented at high magnification in Figures 1h and 3. The latter suggests that the small (~1 μm) droplets adhere to the boundary, presumably to the surfactant layer, of the larger one. Due to high water volume fraction, ϕ = 0.807, these emulsions can be characterized as concentrated ones, where one would expect that aggregation plays an important role in the bulk

https://dx.doi.org/10.1021/acs.langmuir.0c02986
Langmuir 2021, 37, 1725–1742